THE CONTRIBUTIONS OF POLYCOMB REPRESSIVE COMPLEX 2 AND H3K27ME3 IN GENE REPRESSION

by

ANNA V. KULAWIEC

A THESIS

Presented to the Department of Biology
and the Robert D. Clark Honors College
in partial fulfillment of the requirements for the degree of
Bachelor of Science

June 2020

An Abstract of the Thesis of

Anna V. Kulawiec for the degree of Bachelor of Science
in the Department of Biology to be taken June 2020

Title: The Contributions of Polycomb Repressive Complex 2 and H3K27me3 in Gene Repression

Approved: _____*Eric U. Selker, Ph.D.*_____
Primary Thesis Advisor

Though DNA contains our genes, the expression of genes varies during development and across different cellular conditions. Gene expression can be regulated by the post-translational protein modification of chromatin, such as the trimethylation of lysine 27 of histone 3 (H3K27me3). This mark, catalytically deposited by the protein complex Polycomb Repressive Complex 2 (PRC2), represses associated genes. Such repression is crucial for establishing gene expression patterns for proper development, and aberrant activity of PRC2 can cause disease, such as cancer. Here I present *Neurospora crassa* as a model organism for studying the repressive effects of PRC2, independent of its catalytic mark, H3K27me3. I generated a catalytically inactive SET-7, the catalytic component of PRC2 in *N. crassa*, demonstrating that elimination of H3K27me3 is sufficient to depress genes it normally marks despite the physical presence of PRC2. I further show that, in contrast to SET-7 knockout, catalytic inactivation of SET-7 does not alter the stability of PRC2. Moreover, catalytic inactivation of SET-7 enriches a higher molecular weight form of the core PRC2 member SUZ12. Overall, this work indicates that the physical form of PRC2 in itself does not act repressively and suggests that studies focusing on its repressive effects should consider that methods of H3K27me3 elimination, either knockout or catalytic inactivation, differentially affect PRC2 complex stability.

Acknowledgements

I would like to express my sincere gratitude to Dr. Eric Selker. He provided me with the opportunity to delve headfirst into research and fostered enthusiasm for my project, all while offering the independence I didn't know I needed to learn and thrive. I am exceedingly indebted to my mentors, Dr. Tereza Ormsby and Dr. Vincent Bicocca. Tereza, willing to take a chance on a novice, was instrumental in cultivating my excitement for this research. As we developed this project, Vince pushed me outside of my intellectual comfort zone, but through this, I saw how much I could achieve.

I wish to warmly thank William Stork for serving as my second reader, his indispensable daily advice, and his thoughtful encouragement all these years. Thank you to the rest of the Selker lab, Dr. Jeanne Selker, Dr. Tish Wiles, and Dr. Kevin McNaught, for their guidance and kindness.

I would also like to thank Dr. Daphne Gallagher for her active participation as my CHC representative. She has been a rational and confidence-instilling sounding board amidst my research ups and downs, and for her I am extremely grateful. Additionally, thank you to Karl Reasoner and the individuals of the VPRI Undergraduate Fellowship, as well as the individuals of the CHC Schwartzrock Family Thesis Research Grant, for making full time work on my research project possible.

And finally, thank you to my family and friends. Their feedback, patience, and encouragement mean the world to me.

Table of Contents

List of Figures

List of Tables

Introduction

DNA Packaging and Epigenetics

Similarly to how a cookbook contains a complete set of recipes, each cell's DNA contains the complete set of genomic instructions necessary for life. However, we only prepare a few recipes from a cookbook at a time, akin to how different cells from different tissues require only a subset of genes to be active at a given time. Cells must therefore find ways to regulate patterns of gene expression while packaging DNA into a compact form within the nucleus.[1] A mechanism of regulating gene expression and compacting DNA is the evolution of nucleosomes in eukaryotes. Strands of DNA wrap around a core of histone proteins, and DNA-histone bundles form nucleosomes (Fig. 1A).[2] Nucleosomes, along with other molecules, bundle to form chromatin, and this compaction affects DNA accessibility and thus gene expression (Fig. 1B).[2] Epigenetic modifications, ones that are associated with heritable and semi-heritable changes in gene expression, can alter the organizational structure of chromatin and thus change gene expression. One type of an epigenetic modification is the addition of various chemical groups to the histones within nucleosomes, and this significantly affects the expression of the underlying DNA.[2-5]

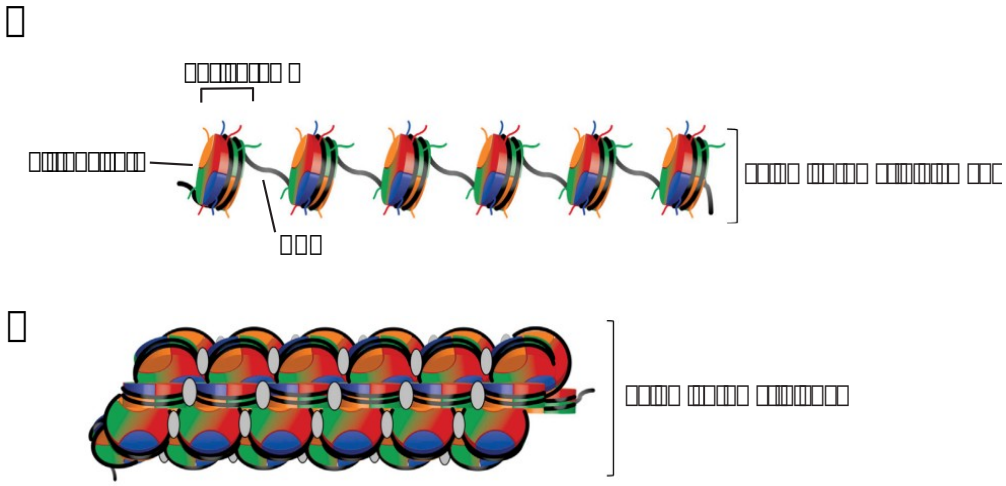

Figure 1. The structure of nucleosomes and chromatin. (A) DNA wraps around a histone core, forming a nucleosome. The 10 nm chromatin filament represents a less compact, and thus more accessible, form of chromatin. (B) Different forms of nucleosome bundling affect DNA accessibility through compaction of chromatin structure. Greater bundling, such as in the 30 nm fiber, is associated with decreased DNA accessibility.[2] Figure adapted from Gross et al., 2015.[1]

Gene Repression by PRC2 and H3K27me3

An important example of this type of modification is methylation of the amino acid lysine (K) 27 of histone H3 (H3K27me), a widely conserved mark.[7] Lysines are able to bear up to three methyl groups simultaneously, and all three forms (mono- (H3K27me1), di- (H3K27me2), and trimethylation (H3K27me3)) are thought to be biologically significant.[6] Repression by H3K27me1 is associated with regions of active gene transcription, whereas H3K27me2 is thought to act as a "placeholder" before H3K27me3 in embryonic stem cells, preventing other forms of post-translational modifications.[6] Trimethylation of H3K27 (H3K27me3) is a repressive mark that is critical for embryonic development and is involved in the silencing of associated

genes.[4, 7] H3K27me3 is thought to act repressively by serving as a docking site for effector proteins.[1]

Polycomb Repressive Complex 2 (PRC2) catalyzes the deposition of H3K27me3 and localizes to the promoters of lowly transcribed and inactive genes (Fig. 2).[7-9] This complex exhibits greater activity in regions of dense oligonucleosomes *in vitro*, suggesting that it localizes to compact chromatin states and contributes to gene inactivation.[10]

PRC2 has three core components: EZH2 (SET-7 in *N. crassa*), EED, and SUZ12, all of which are conserved and crucial for establishing H3K27me3 patterns genome-wide (Fig. 2).[4, 7] EZH2 contains a conserved catalytic SET domain that transfers methyl groups to lysine 27 of histone H3, depositing the repressive mark.[4, 7] Two characteristic regions in the SET domain are the AdoMet binding pocket and the target tyrosine residue adjacent to the F/Y switch.[4] The AdoMet binding pocket contains the methyl group to be transferred to the histone during methylation, and the target tyrosine residue coordinates the target lysine to receive methylation.[3, 4] Although contact with SUZ12 and EED are important for PRC2 recruitment, stability, and activity,[9, 11] the SET domain only minimally requires EED and the VEFS domain (the domain that binds EZH2) of SUZ12 for catalytic activity.[12] However, the association between each of these subunits confers stability to the PRC2 complex as a whole,[12] and in the absence of the other PRC2 core subunits, EZH2 is autoinhibited.[9] It has been shown, however, that catalytic inactivation of EZH2 maintains PRC2 complex assembly.[13] After EZH2 deposits H3K27me3, EED can bind to the deposited H3K27me3 and induce a conformational change in EZH2 that enhances its ability to further deposit H3K27me3,

creating feedback mechanism that results in the “spreading” of H3K27me3 to neighboring nucleosomes.[9] Additionally, the SUZ12 subunit is important to PRC2 function, as it both stabilizes EZH2 and can be recruited to other target loci.[9, 14]

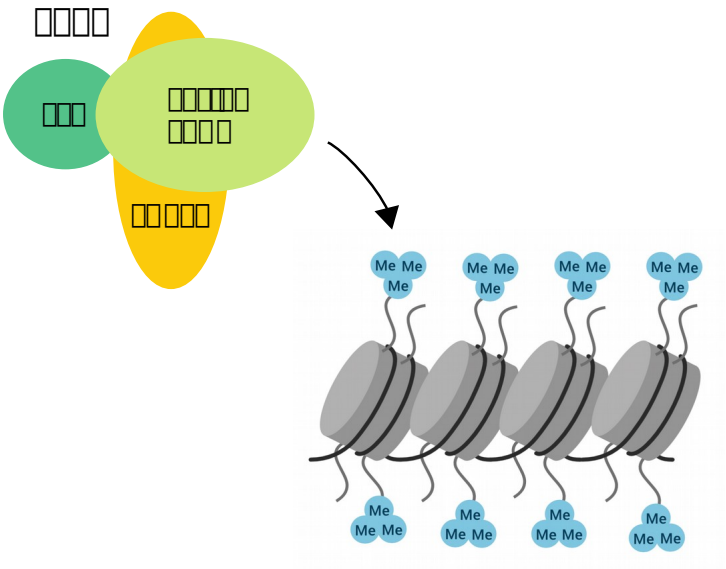

Figure 2. Deposition of H3K27me3 by PRC2 in the fungus *Neurospora crassa*. Figure was adapted from Laugesen et al., 2019.[15]

These core subunits are not the only subunits associated with PRC2, and studies have shown that accessory PRC2 subunits engage in distinct forms of PCR2 complexes, named PRC2.1 and PRC2.2 (Fig. 3).[9, 16] PRC2.1 contains proteins that are thought to be involved in localization to particular regions of chromatin, whereas subunits in PRC2.2 have been shown to catalytically activate, recruit, and possibly stabilize EZH2.[9, 11] Although these forms of PRC2 are distinct, current models support the hypothesis that the accessory proteins to PRC2 cooperatively direct H3K27me3.[11]

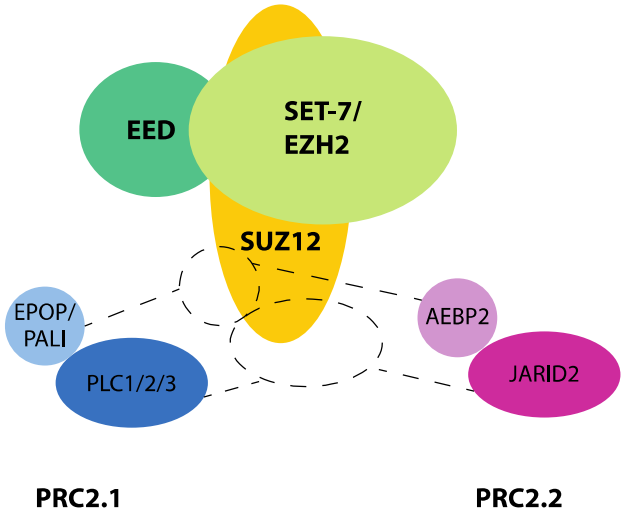

Figure 3. Schematic of two distinct forms of PRC2 complexes, PRC2.1 and PRC2.2.The potential binding sites for non-core complex members are indicated. EPOP/PALI and PLC1/2/3 are thought to be the accessory subunits in PRC2.1, and AEBP2 and JARID2 are thought to be the accessory subunits in PRC2.2. Figure was adapted from Laugesen et al., 2019.[15]

Nevertheless, because PRC2 deposits H3K27me3, it is unclear if H3K27me3 is *solely* responsible for repression, or if the presence of the protein complex also plays a repressive role. This project seeks to determine if the physical presence of PRC2 is also involved in repression, independent of its catalytic mark.

PRC2 and H3K27me in Development and Disease

Given the importance of PRC2 and H3K27me in gene expression, it is unsurprising that these epigenetic factors are implicated in various developmental problems and diseases. PRC2 and H3K27me are widely conserved, existing in organisms from humans to fungi, indicating the critical role it plays in gene expression.[7] Research in mice has shown that EZH2 regulates growth control for mouse embryonic

development, and mutations in EZH2 result in severe impairment of mouse cell differentiation.[17] Other subunits of PRC2, namely EED and SUZ12, are also critical for embryonic development.[8, 13] In addition to development, dysfunction of these factors also plays a role in cancer etiology, demonstrating their significance for appropriate long-term gene expression patterns.[7] For example, Diffuse Intrinsic Pontine Glioma is an aggressive type of pediatric brainstem tumor associated with a reduction of H3K27me3, suggesting abnormal PRC2 activity contributes to cancerous growth.[18] Additionally, dysfunction of the PRC2 subunit of EZH2 is involved in prostate and breast cancer.[4, 19] Together, the developmental defects and cancerous outcomes for dysregulation of PRC2 and H3K27me demonstrate the vital need for further research into these epigenetic factors.

Neurospora crassa as a Model Organism

The filamentous fungus *Neurospora crassa* is a valuable model organism, as it grows quickly, contains a small haploid genome, is well defined, and is genetically tractable (Fig. 4).[20] *N. crassa* hosts a variety of epigenetic modifications and mechanisms.[21] Similar to other eukaryotic organisms such as mammals, flies, and plants, *N.crassa* contains H3K27me3, and genes with this mark are normally silent.[20] Though the catalytic component of PRC2 in *N. crassa* is SET-7, this protein behaves like EZH2 in other organisms, and both can be considered equivalent. SET-7, like EHZ2 in animals, contains the SET domain that transfers methyl groups to specific lysine residues.[4, 7] Although disruptions to PRC2 and H3K27me in other organisms lead to developmental defects, interestingly, these epigenetic factors are dispensable for

normal growth and developmentin *N. crassa*.[7] Thus, *N. crassa* is well suited for studying PRC2 and its catalytic mark, as others have shown,[5]as these epigenetic factors may be altered or removed to study resulting changes without killing the organism.

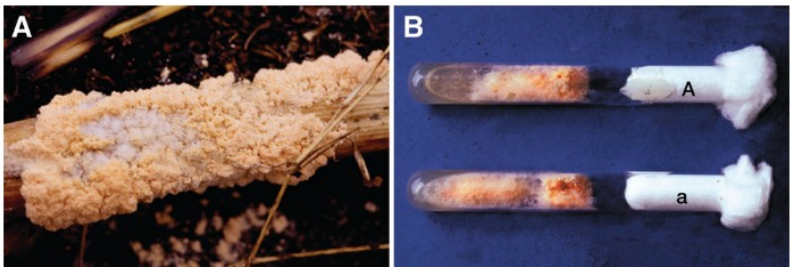

Figure 4. Images of *Neurospora crassa*. (A) Wild growth on sugarcane. (B) Laboratory growth in slants. Figures were adopted from Aramayo and Selker, 2013.[20]

Current Understanding of PRC2 and H3K27me3 Repression

Although it is currently understood that H3K27me3 is a repressive mark deposited by PRC2, much remains unknown about the repressive mechanism of this complex and its mark. The different methylation states of H3K27 are associated with different patterns in gene expression.[8] Furthermore, the ways in which different histone modifications influence each other and gene expression remain active points of research.[2, 22] For example, it was recently discovered that PRC2 has a "sensing pocket" that recognizes the unmodified histone H3 lysine 36 (H3K36) residue,[23] demonstrating interactions between PRC2 and histone residues. Methylation of H3K36 is normally associated with active transcription, but it has been found to localize near H3K27me3 at poorly transcribed genes, further indicating the complex interplay between histone modifications and gene expression.[2, 24] Although H3K27me3 is associated with silenced

genes, a “reader” of H3K27me3 in *N. crassa* has been shown to act repressively, suggesting that H3K27me3 alone does not repress genes.[25]

Thus, a gap in understanding remains regarding the role of the physical complex of PRC2 in gene repression, independent of its catalytic mark. My project therefore seeks to investigate the individual contributions of H3K27me3 and the PRC2 complex in gene repression. By inactivating SET-7, the catalytic component of PRC2 in *N. crassa*, I sought to eliminate H3K27me3 but retain the physical integrity of PRC2. This allowed to me differentiate between PRC2 and its catalytic mark and gain understanding of the role PRC2 may play in gene repression, independent of this mark. I divided this researchinto three primary objectives.

Objective 1: Mutant Construction to Eliminate H3K27me3

To eliminate the deposition of H3K27me3 by PRC2, conserved residues in SET-7 predicted to be essential for catalysis were substituted with biochemically similar amino acids that would eliminate catalytic activity. The amino acid tyrosine (Y) contains a phenol group in its sidechain, and Y833 of the SET domain is conserved throughout animals and other fungi. Y833 coordinates the target lysine of histone H3 through hydrogen bonds between the target lysine and the hydroxyl group of the tyrosine sidechain (Fig. 5A).[4] By substituting this tyrosine with a phenylalanine (F) amino acid (Y833F), which is similar in size but lacking the hydroxyl group, I aimed to eliminate the coordinating activity of Y833.

An additional catalytic mutation was made at histidine (H) 791 of SET-7. H791 is crucial to the pseudoknot fold of the SET domain, forming an active site adjacent to

where the methyl donor binds, allowing for methylation of the histone substrate (Fig. 5B).[4] Destruction of the pseudoknot fold has been shown to eliminate methyltransferase activity in human cells.[4] A similar strategy was employed in *N. crassa* by substituting the catalytically important histidine with an alanine residue, thereby decreasing the size and eliminating possible hydrogen bonds.

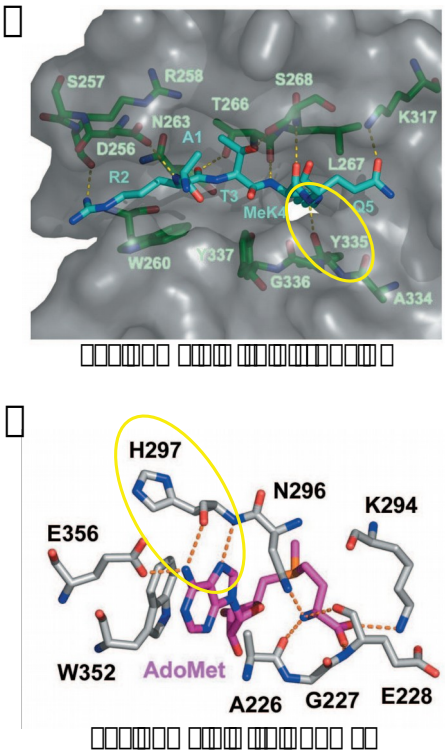

Figure 5. The conserved catalytic SET domain.Residues and their hydrogen bond interactions are outlined in yellow. (A) The conserved tyrosine residue interacting with a lysine residue on the tail of histone H3. (B) The conserved histidine residue interacting with the AdoMet methyl donor. Figure was adapted from Dillon et al., 2005.[4]

One additional SET-7 mutant was constructed to investigate the relative importance of the C-terminus of SET-7. Sequence alignments of SET-7 between model organisms revealed a large unconserved C-terminal extension in *N. crassa* SET-7 (Fig.

6). To study the possible role this C-terminal extension might play in SET-7 activity, SET-7 was truncated at residue 853, after the SET domain.

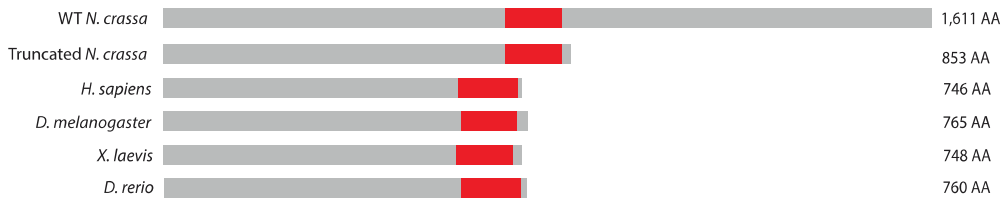

Figure 6. Schematic of SET-7 orthologs. Red regions denote the conserved SET domain.

Objective 2: Assess Repression in SET-7 Mutants

To differentiate between the potential individual contributions of H3K27me3 and PRC2 outside of catalysis in repression, expression of genes normally marked by H3K27me3 was quantified. Although H3K27me3 is repressive, localization of an inactive PRC2 may yet impede transcription by physically blocking transcriptional machinery from reaching DNA. Because genes marked by H3K27me3 exhibit basal levels of expression, increased levels of expression in a catalytic-null SET-7 background would indicate that the structure of PRC2 does not act repressively. No change in expression despite the mutant background, however, would indicate that another factor, such as PRC2, is acting to repress genes despite the absence of H3K27me3.

Objective 3: Assess PRC2 Complex Assembly with Mutant SET-7

Testing my research hypothesis required an evaluation of the complex stability of PRC2 when SET-7 is catalytically inactivated. Previous research showed that point mutations to this catalytic component do not alter interactions of other PRC2 subunits,[26] demonstrating that inactivation of the methyltransferase does not disrupt complex assembly. Identification of changes in PRC2 complex assembly through assessment of PRC2 core subunit protein levels could be used as an indicator of complex assembly. Loss of subunit protein levels, detected by immunoblot signal intensity, would suggest degradation of PRC2 subunits leading to complex instability.

Results

Catalytic-null SET-7 mutations eliminates H3K27me3

In order to eliminate H3K27me3 while maintaining the structure of SET-7, I engineered two catalytic-null *set-7* mutant strains of *N. crassa*. Each strain contained a point mutation in the SET domain, which is critical for SET-7 methyltransferase activity.[4] One mutation was engineered to change a conserved histidine residue of the AdoMet binding pocket of the SET domain into an alanine (H791A) (Fig. 7A). This mutation is predicted to affect SET domain capability to transfer methyl groups on to histone substrate.[4] The second mutation targeted Y833, the tyrosine residue adjacent to the F/Y switch of the SET domain (Fig. 7A). This tyrosine coordinates the target lysine to receive methylation, and mutation of this residue to a phenylalanine (Y833F) likely removes the coordinating hydrogen bond.[2, 4] I confirmed and validated these mutant strains by Sanger sequencing and western blot analysis. Both mutations eliminated H3K27me3, phenocopying a Δ*set-7* strain (Fig. 7B). These data demonstrate that Y833F and H791A mutations catalytically inactivate SET-7.

SET-7 C-terminus is not required for H3K27me3

To explore the functional importance of regions besides the SET domain, I truncated the C-terminus of SET-7 at residue 853, removing a segment of the methyltransferase immediately following the evolutionary conserved SET domain. Western blot analysis revealed retention of H3K27me3 in *set-7*$^{1\text{-}853}$ strains, suggesting that the C-terminus of *set-7* is dispensable for H3K27me3 deposition in *N. crassa* (Fig.

7B). In contrast to the wild-type truncation, strains containing both the truncation and catalytic mutation exhibited a loss of H3K27me3, identical to Δ*set-7*strains (Fig. 7B). Together, these results indicate that the SET domain, but not the C-terminus, is required for deposition of H3K27me3.

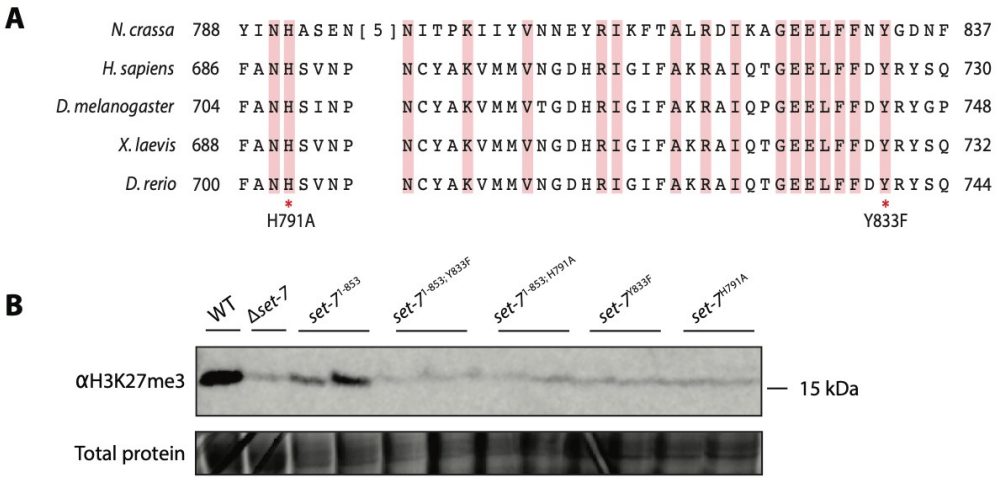

Figure 7: Mutation, but not truncation, of SET-7 results in loss of H3K27me3. (A) Sequence alignment of the SET domain of SET-7 orthologs containing the AdoMet histidine (H791) and target tyrosine (Y833). (B) Western blot analysis for H3K27me3 in engineered mutant strains, with total protein loaded visualized by exposure to UV light.

Catalytic-inactivation of SET-7 derepresses an H3K27me3-marked gene

To investigate if the loss of SET-7 catalytic activity alone derepresses genes marked by H3K27me3, I tested for increases in expression of genes silenced by H3K27me3.[27] The gene *NCU07152* is marked by H3K27me3 and is silent under normal conditions.[28] Dr. Elizabeth Wiles, of the Selker group, replaced this gene with *nat-1*, which provides resistance to the antibiotic nourseothricin. Sensitivity to nourseothricin

would demonstrate maintenance of *nat-1* silencing, whereas growth in the presence of nourseothricin would indicate derepression of H3K27me3-marked *nat-1*. The presence of *nat-1* in a wild-type background or catalytic-null *set-7* alone does not allow for growth. However, sibling *set-7*^{Y833F} strains robustly grew on nourseothricin, identical to Δ*set-7* strains (Fig. 8A). This demonstrates that elimination of H3K27me3 alone leads to derepression of an H3K27me3-marked gene, even with the presence of SET-7.

To determine if changes in gene expression generally occurred in other genes marked by H3K27me3, I performed reverse transcriptase quantitative PCR (RT-qPCR) in *set-7* siblings on three additional genes repressed by SET-7. I found that the expression of H3K27me3-marked genes consistently increased in *set-7*^{Y833F}and Δ*set-7* strains. The expression of *NCU05173* increased by 213% relative to wild type in *set-7*^{Y833F} strains and by 231% in *set-7*$^{1-853;\ Y833F}$strains (Fig. 8B). These increases in gene expression exceed that observed in Δ*set-7* strains, which displayed an increase in expression of *NCU05173* of 143% relative to wild type. I observed similar increases in expression for *NCU07152*, with *set-7*^{Y833F} exhibiting a 665% increase, *set-7*$^{1-853;\ Y833F}$ exhibiting a 431% increase, and Δ*set-7* exhibiting a 224% increase relative to wild type. However, there were only modest increases in expression of *NCU09640*: the *set-7*^{Y833F} mutation increased expression by 3.01%, *set-7*$^{1-853;\ Y833F}$by 4.58%, and Δ*set-7* by 2.52% relative to wild type. Truncated SET-7 only slightly increased *NCU05173*, *NCU07152*, and *NCU07624* expression (Fig. 8B), consistent with the retention of H3K27me3 in this strain (Fig. 8B). Interestingly, in *NCU07624*, this increase of expression was greater than in any mutant *set-7* strain, with an 8.93% increase compared to the 6.23% increase of Δ*set-7* strains, 7.48% of *set-7*^{Y833F}strains, and 8.28% increase of *set-7*$^{1-853;\ Y833F}$strains.

In contrast, truncated *set-7* did not increase the expression of *NCU09640*, with 0.386% decreased expression of this gene. Altogether, these data demonstrate a general increase of expression of H3K27me3-silenced genes when SET-7 is inactivated.

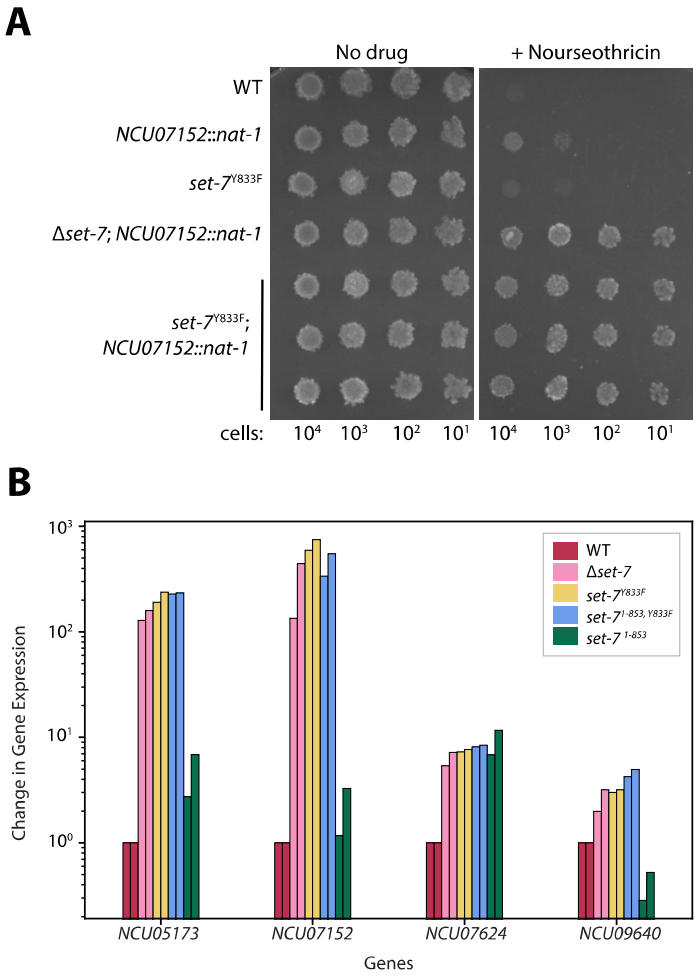

Figure 8: Catalytic-inactivation of SET-7 derepresses H3K27me-3 marked genes. (A) Serial dilution spot test silencing assay for the indicated strains on the indicated media. (B) RT-qPCR results for the indicated genes, normally repressed by SET-7 activity. Duplicate bars represent duplicate samples of the indicated strains.

Mutant *set-7* retains levels of EED while Δ*set-7* decreases EED levels

To investigate the potential effects of the catalytic-null SET-7 on PRC2 complex assembly, I assessed the stability of other core PRC2 components, EED and SUZ12, through western blot analysis. Loss of core members could indicate protein instability and faulty PRC2 complex assembly.[13] Strains containing C-terminal 3xFLAG-tagged EED in either a Δ*set-7* or *set-7*^{Y833F} background were assessed by western analysis, immunoblotting for enrichment of EED-3xFLAG (Fig.9A). The relative intensities of the EED bands were calculated by normalizing intensity to PGK1 levels (a loading control). Control strains without the FLAG tag showed only background signal intensity. Interestingly, *set-7*^{Y833F}retained EED levels, with a 10.5% increase in EED signal intensity. In contrast, Δ*set-7* showed a 26.5% reduction in EED (Fig. 9B). This suggests that the presence of SET-7 maintains EED stability, even with the loss of catalytic activity.

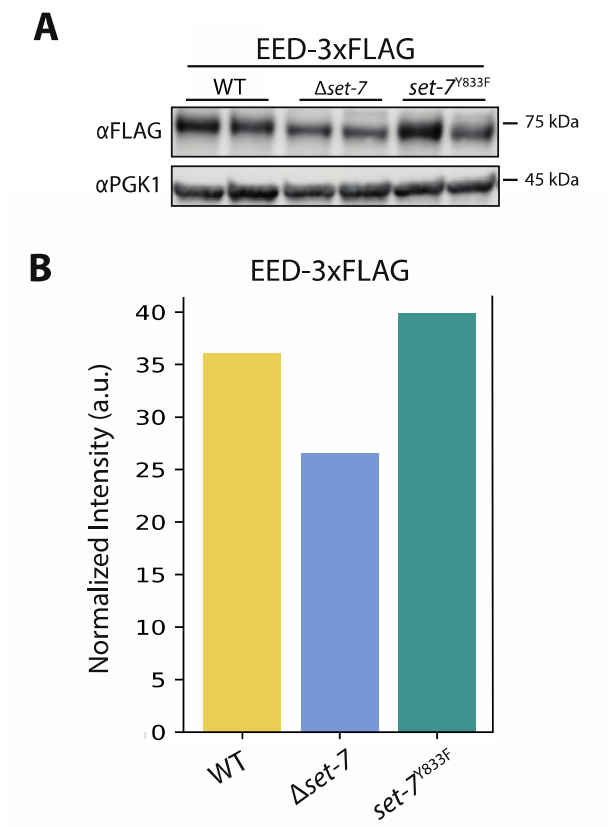

Figure 9: Catalytic-inactivation of SET-7 retained levels of EED. (A) Western blot analysis of the indicated *N. crassa* strains, probing for levels of EED::3xFLAG and PGK1, a housekeeping gene. (B) Quantification of relative band intensity of indicated *N. crassa* strains from Figure 7A, normalized to PGK1 levels. "a.u." indicates arbitrary units. Duplicates were averaged and the intensity of the wild type average was set to 1.

Mutant SET-7 increases levels of higher molecular weight SUZ12 but decreases levels of lower molecular weight SUZ12

I further analyzed PRC2 stability by assessing levels of SUZ12 in mutant *set-7* and Δ*set-7* backgrounds. Strains with C-terminally tagged *suz12* in either Δ*set-7* or *set-7*^{Y833F} backgrounds were assessed by western blot analysis in duplicate, probing for

levels of SUZ12::3xFLAG (Fig. 10A). Wild-type SUZ12 exhibits two molecular weight bands, of sizes near 97 kDa. I found that the presence of *set-7*^{Y833F}or Δ*set-7* enriched the higher molecular weight band of SUZ12 but depleted the lower molecular weight band. The relative intensities of the SUZ12 bands were calculated by normalizing intensity of SUZ12 bands to PGK1levels. The intensity of the higher molecular weight band of SUZ12::3xFLAG in *set-7*^{Y833F} was 3.98-fold greater than the intensity of *suz12*, indicating enrichment of this form of SUZ12. Such enrichment also occurred in Δ*set-7*, although to a lesser extent than the mutant methyltransferase, with 1.66-fold greater intensity (Fig. 10B).

Comparison of ratios of signal intensity between the bands of SUZ12 also revealed that the higher molecular weight band of SUZ12 became similarly enriched in both Δ*set-7* and *set-7*^{Y833F} strains. The signal intensity ratio of higher molecular weight marker/lower molecular weight marker was 0.375, 2.09, and 1.80 in wild type, Δ*set-7*, and *set-7*^{Y833F} strains, respectively (Fig. 10C). Wild type SUZ12 exhibited a greater signal intensity for the lower molecular weight band, as this lower band's intensity was 2.66-fold greater than the higher band (Fig. 10B). In contrast, Δ*set-7* and *set-7*^{Y833F} strains exhibited a greater signal intensity for the higher molecular weight band of SUZ12 than the lower band, resulting in a greater ratio of higher molecular weight marker/lower molecular weight marker signal intensity (Fig. 10C). However, compared to wild type, the total SUZ12 intensity was not maintained in the Δ*set-7* and *set-7*^{Y833F} strains. Wild type strains exhibited a total SUZ12 signal intensity of 1.51 a.u., whereas Δ*set-7* and *set-7*^{Y833F} strains exhibitedtotal intensities of 1.02a.u. and 2.56 a.u., respectively (Fig. 10C). This resulted in a 32.8% decrease in total SUZ12 intensity in

Δ*set-7* strains but a 169% increase in signal in *set-7*^{Y833F} strains (Fig. 10C). Thus, the change in signal intensity ratio, though similar for Δ*set-7* and *set-7*^{Y833F} strains, resulted from differing changes in signal intensity of each SUZ12 band. Whereas the signal of the lower molecular weight band of SUZ12 in *set-7*^{Y833F} strains slightly decreased, with 17.0% decreased intensity of *set-7*^{Y833F} SUZ12 compared to wild type, Δ*set-7* exhibited far greater reduction in intensity of SUZ12, with a 70.0% reduction. In summary, these data suggest that alteration of *set-7* affects the stability of SUZ12. Mutation of *set-7* enriches the higher molecular weight band of SUZ12, yet the elimination of *set-7* greatly reduces the quantity of lower molecular weight SUZ12 compared to mutated *set-7*.

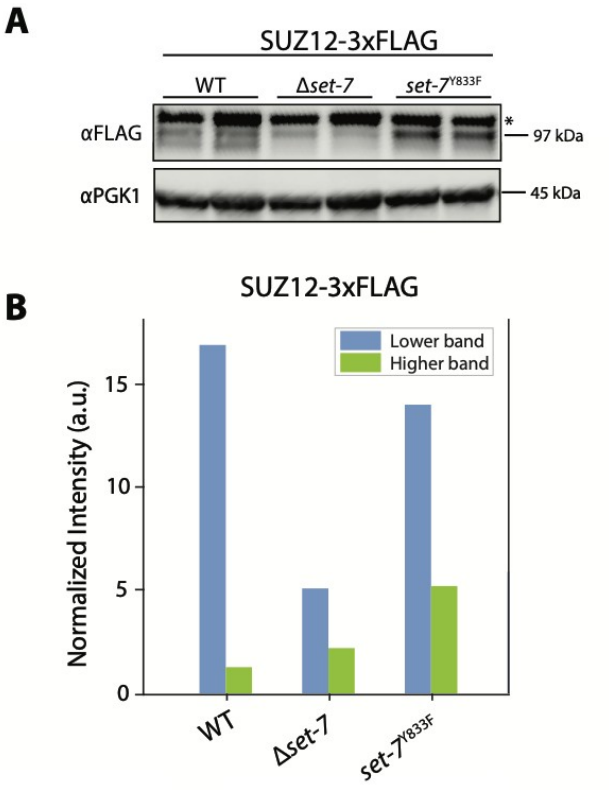

C

Sample	Band	Normalized Signal (a.u.)	Sum	Ratio High/Low
WT	High	0.413	1.51	0.375
	Low	1.100		
Δset-7	High	0.687	1.02	2.09
	Low	0.329		
set-7^{Y833F}	High	1.647	2.56	1.80
	Low	0.916		

Figure 10: Catalytic-inactivation of SET-7 increasedlevels of higher molecular weight SUZ12 and reducedlevels of lower molecular weight SUZ12. (A) Western blot analysis of the indicated *N. crassa* strains, probing for levels of SUZ12::FLAG and PGK1, a housekeeping gene. * indicates a nonspecific band. (B) The relative intensity of the higher molecular weight SUZ12 band in indicated strains, normalized to PGK1. “a.u.” indicates arbitrary units. Duplicates were averaged, and the intensity of the wild-type average was set to 1. (C) The normalized signal of each SUZ12 band in the indicated samples, as well as the sum of signal intensity and ratio of signal intensity between the high and low molecular weight bands of SUZ12.

Discussion

Although it is well-established that H3K27me3 is a repressive mark deposited by SET-7,[7] previous methods for studying H3K27me3 through *ezh2/set-7* knockouts introduced two variables that could influence PRC2-mediated repression: elimination of H3K27me3 and potential destabilization of PRC2. Though it is known that SET domain knockouts can destabilize PRC2 complex member associations in mouse embryonic stem cells,[29] the effect of a *set-7* knockout compared to a catalytically-inactive*set-7* on complex stability and gene repressionrequires further investigation. Here, I have characterized how catalytic-inactivation of the H3K27 methyltransferase affects gene repression and PRC2 complex stability in *N. crassa*.

An important conclusion of this work is that PRC2 does not repress genes independently of its catalytic mark, H3K27me3. Consistent with other work,[2] the loss of methyltransferase activity through mutations to the SET domain eliminated H3K27me3. This loss is sufficient to derepress genes marked by H3K27me3, suggesting that the presence of PRC2 alone is insufficient for repression. Western blot analysis of core PRC2 components, EED and SUZ12, suggested that loss of *set-7* destabilizes PRC2, whereas catalytic inactivation of the methyltransferase maintains the complex. Loss of *set-7* reduced the signal intensity of EED by 26.5% and reduced the total SUZ12 signal by 32.8%, indicating that Δ*set-7* destabilizes PRC2. Destabilization of PRC2 through deletion of *set-7* is consistent with previous research in mouse embryonic stem cells,[29] and thus, it is unsurprising that Δ*set-7* strains exhibit reduced immunoblot intensity of PRC2 core components (Fig. 9A and Fig 10A). In contrast, *set-7*^{Y833F} retained EED levels, suggesting that the presence of SET-7 is sufficient to maintain EED stability.

Moreover, catalytic-null *set-7* increased the total signal intensity of SUZ12 by 169%, with an enrichment in the higher molecular weight form SUZ12. Thus, it appears more likely that catalytic-null *set-7* maintains the stability of PRC2 while favoring the higher molecular weight form of SUZ12.

It would be interesting to investigate why catalytic-null *set-7*enriches this higher molecular weight SUZ12 form. While further research into the functional importance of the differently sized SUZ12 proteins is necessary, it is possible that *suz12* contains two transcriptional start sites, and each of the SUZ12 molecular weight bands correspond to two different sizes of SUZ12 protein. It is known that the N-terminus of SUZ12 binds the target regions for PRC2 and localizes PRC2 to correct genomic loci,[29] yet it remains unknown if a different isoform of SUZ12 is involvedin this localization. The case could be such that deletion of *set-7* destabilizes all forms of SUZ12, whereas loss of H3K27me3 but retention of SET-7 enriches the higher molecular weight form of SUZ12, which may be present in only a subset of PRC2 complexes. Another possible explanation may be that *suz12* is alternatively spliced, with variation in forms depending on the H3K27 methylation state. The *suz12* gene is also marked by H3K27me3 (W. Storck, personal communication), and perhaps the presence of H3K27me3 facilitates the production of the lower molecular weight SUZ12 by the alternative splicing of *suz12*. Lastly, SUZ12 could preferentially receive post-translational modifications of mutant *set-7* strains that increase the apparent weight of its molecular weight band. The existence of these two forms of SUZ12 could be evaluated by comparing mass spectrometry samples of each form to their predicted protein size, based on possible alternative splicing patterns and start codons for SUZ12.

Additional research into these forms of SUZ12 could help illuminate the mechanisms of PRC2 localization and complex forms.

Further steps in this inquiry are necessary to elucidate the interplay between catalytic-nullSET-7 and PRC2 subunits. Co-immunoprecipitation between EED and SUZ12, a method to determine if the two proteins bind to each other, in Δ*set-7* and catalytic-null *set-7* backgrounds could further demonstrate PRC2 complex stability if the proteins retain normal binding, despite a mutant background. Additionally, chromatin-immunoprecipitation with mutant SET-7, EED, and SUZ12 may reveal if the methyltransferase and other PRC2 subunits interact with normal target genomic regions, indicating that the catalytic-null PRC2 complex correctly localizes despite loss of methyltransferase activity.

Although catalytic-null *set-7* derepresses H3K27me3-marked genes similarly to Δ*set-7*-induced derepression, my results indicate that studies involving H3K27me3 should take care in eliminating this catalytic mark. Because catalytic-null *set-7* appears to alter PRC2 by enriching the larger molecular weight form of SUZ12 and loss of SET-7 destabilizes the entire complex, elimination of H3K27me3 by *set-7* deletion or *set-7* mutation will have different effects on PRC2 stability. Importantly, my research suggests that catalytic-inactivation of *set-7* may be a better model for eliminating H3K27me3 than deletion of *set-7*, as the mutation of the methyltransferase does not decrease PRC2 stability as severely as Δ*set-7*.

Materials and Methods

N. crassa strains, media, and growth conditions

Table 1 lists the *N. crassa* strains used in this study. *N. crassa* strains were grown, maintained, and crossed according to standard procedures.[30, 31] Spot tests of *N. crassa* strains, to verify genotype and to assess changes in gene expression, were performed at 32˚C on Vogel's minimal medium with 0.8% sorbose, 0.2% fructose, and 0.2% glucose (FGS) medium plates for 3 days.[30] When tests included antibiotic resistance, plates also included 200 µg/mL Hygromycin B Gold (InvivoGen), 133 µg/mL Nourseothricin (Gold Biotechnology), or 10 µg/mL glufosinate ammonium (Bayer) as appropriate.[25] The methods for isolating genomic DNA were performed as previously described.[32]

Endogenous C-terminal-tagging of SET-7 with 3xFLAG::hph

The 3' end of the *set-7* ORF was PCR-amplified from wild-type genomic DNA using primers 4108 and 4109, and the *set-7* 3' flank was PCR-amplified from wild-type genomic DNA using primers 4110 and 4111. The *set-7* ORF PCR-product and the *set-7* 3' flank PCR product were separately stitched to plasmid 2409 (source of 3xFLAG::*hph*) via PCR, using primers 4108 and 2955, and 2954 and 4111, respectively. The resulting two "split-marker" PCR products were co-transformed into N2931 and transformants containing mutant *set-7*::3xFLAG::*hph* constructs were selected on hygromycin-containing medium.

Site-directed mutagenesis

To generate a mutant H791 SET-7 retaining amino acids 1-853, the 5' (upstream region) and 3' (downstream region) mutant flanks were PCR-amplified from wild-type genomic DNA using primer pairs 6469 and 6562 (5') and 6561 and 6470 (3') (see Table 2). The 5' and 3' flanks were PCR-stitched together using primers 6469 and 6470. To add 3xFLAG::*hph*, the mutant fragment was PCR-stitched to plasmid 2409 (source of 3xFLAG::*hph*, see Table 3) using primers 6469 and 2955. To add the *set-7* 3' UTR to the mutant fragment, the 3' UTR mutant flank of *set-7* was PCR-amplified using primers 6561 and 4109. The 3' mutant flank and mutant fragment were PCR-stitched together using primers 6469 and 4109. To extend the complete mutant construct, the construct was PCR-stitched to plasmid 2409 using primers 6469 and 2955. The 3'*set-7* UTR was PCR-amplified from wild-type genomic DNA with primers 4110 and 4111. This PCR product was PCR-stitched to plasmid 2409 to generate a 3xFLAG::*hphset-7* 3' UTR construct. This split-marker PCR product was co-transformed with the mutant *set-7* fragment into strain N2931 and mutant *set-7*::3xFLAG::*hph* constructs were selected on hygromycin-containing medium. The co-transformation and selection were also performed with the mutant C-terminally truncated *set-7* fragment. *set-7*$^{1\text{-}853,\ H791A}$ primary transformants were confirmed by Sanger sequencing using primers 6469, 2955, and 5611 to verify that H791 was mutated. *set-7*$^{1\text{-}853,\ H791A}$ primary transformants were then crossed to N3752 to generate N8177 and N8178. *set-7*$^{1\text{-}853}$ primary transformants were crossed to N3751 to generate N8157 and N8158. *set-7*^{H791A} primary transformants were subjected to Sanger sequencing using primers 6469, 2955, and 1231 to verify that

H791 was mutated. *set-7*^{H791A} primary transformants were then crossed to N3752 to generate N8163 and N8164.

To generate a mutant C-terminally truncated *set-7* fragment retain amino acids 1-853, the 5' (upstream region) and 3' (downstream region) mutant flanks were PCR-amplified from wild-type genomic DNA using primer pairs 6469 and 6564 (5') and 6563 and 6470 (3'). The 5' and 3' flanks were PCR-stitched together using primers 6469 and 6470. To add 3xFLAG::*hph*, the mutant fragment was PCR-stitched to plasmid 2409 (source of 3xFLAG::*hph*) using primer pairs 6469 and 2955. To generate a mutant *set*-7 fragment, 3' UTR mutant flank of *set-7* was PCR-amplified using primers 6563 and 4109. The 3' mutant flank and mutant fragment were PCR-stitched together using primer pairs 6469 and 4109. To add the 3xFLAG::*hph* epitope, the mutant fragment was PCR-stitched to plasmid 2409 using primers 6469 and 2955. The 3'*set-7* UTR was PCR-amplified from wild-type genomic DNA with primers 4110 and 4111. This PCR product was PCR-stitched to plasmid 2409 to generate a 3xFLAG::*hphset-7* 3' UTR construct. This "split-marker" PCR product was co-transformed with the mutant *set-7* fragment into strain N2931 and transformants containing mutant *set-7*::3xFLAG::*hph* constructs were selected on Hygromycin-containing medium. The co-transformation and selection were also performed with the mutant C-terminally truncated *set-7* fragment. *set-7*$^{1\text{-}853,\ Y833F}$ primary transformants were confirmed by Sanger sequencing using primers 6469, 2955, and 5611 to verify that Y833 was mutated. *set-7*$^{1\text{-}853,\ Y833F}$ primary transformants were then crossed to N3752 to generate N8159 and N8160. *set-7*^{Y833F} primary transformants were subjected to Sanger

sequencing using primers 6469, 6491, and 1231 to verify that Y833 was mutated.*set-7*^{Y833F} primary transformants were then crossed to N3752 to generate N8161 and N8162.

Transformation into *N. crassa*

To integrate the *set-7*::3xFLAG::*hph* construct into the *set-7* locus in *N. crassa*, the N2931 strain was electroporated, and the sequence was inserted by subsequent homologous recombination.[33] To select for growth of the correct progeny, transformed conidia were plated on hygromycin-containing medium, then incubated at 32ºC for 3 days. Twenty transformants from each construct were randomly selected, and correct integration was validated by Southern analysis.

Southern analysis of genotype

Methods for isolation of genomic DNA and Southern hybridization were employed as previously described.[34] Progeny containing the *set-7*::3xFLAG::*hph*, *suz12*::3xFLAG::*hph*, and *eed::*3xFLAG::*hph* markers were identified by Southern analysis. Genomic DNA samples were digested with EcoRV-HF restriction enzyme (New England Biolabs) overnight at 37˚C with 2 µg of genomic DNA and 40 units of EcoRV restriction enzyme. Digested DNA was visualized with an hph probe labeled with ^{32}P. Probes were constructed from genomic DNA by PCR, with primer pairs 2954 and 397 (Table 4). Due to differential EcoRV-HF cut sites in *set-7*, *suz12*, and *eed*, the presence of the *hph* markers in progeny were distinguishable.

Western blotting to detect H3K27me3 and the FLAG epitope

N. crassa conidia were inoculated in Vogel's minimal medium with 1.5% sucrose for 16 hours while shaking at 32˚C. Tissue was collected by and suspended in 500 µL of ice-cold lysis buffer (50 mM HEPES [pH 7.5], 150 mM NaCl, 10% glycerol, 0.02% NP-40, 1 mM EDTA) supplemented with 1x HaltTM Protease Inhibitor Cocktail (Thermo Scientific). Tissue was sonicated (Branson Sonifer-450) for 2 sets of 20 pulses (Output = 2, Duty cycle = 80), and the samples rested on ice between sets. Samples were centrifuged at 14,000 RPM at 4˚C for 10 minutes to pellet insoluble material, and the supernatant used in the western analysis, including appropriate controls of housekeeping genes and lysate dilutions.[25] Anti-H3K27me3 (Cell Signaling Technology, 9733) and anti-PGK (Abcam, ab38007) primary antibodies were used with IRDye 680RD goat anti-rabbit secondary (LI-COR, 926-68071). Anti-FLAG M2 Peroxidase (HRP) (Sigma, A8592) primary antibody was used with SuperSignal West Femto Maximum Sensitivity Substrate. Images of the western membranes were acquired with an Odyssey Fc Imaging System (LI-COR) and analyzed with Image Studio software (LI-COR).

RNA Isolation and cDNA Synthesis

Germinated conidia were grown for 16-18 hours and added to a 1:1:1 glass beads, NETS (300mM NaCl, 1mM EDTA, 10mM Tris-HCl, 0.2% SDS), acid phenol: chloroform (5:1, [pH 4.5]) mixture. RNA was extracted from this mixture using a bead beater, and ethanol precipitated the RNA. To remove residual DNA, RNA was treated with DNAse I (Amplification grade; Thermo Fischer Scientific). The SuperScript III

First Strand-Synthesis System (Thermo Fischer Scientific) with poly-dT primers was used to synthesize cDNA.

Assessment of Repression by Reverse Transcriptase qPCR

The cDNA generated from RNA isolation and cDNA synthesis was used for qPCR in a Step One Plus Real Time PCR System (Life Technologies) using the PerfCTa SYBR Green FastMix (QuantBio).[25] The primer pairs used are described in Table 4.

Supplementary Information

Table 1. *Neurospora crassa* strains

Strain	**Genotype**
N2931	*mat a; Δmus52::bar; his-3*
N3012	*mat a; Δmus52::bar; his-3*
N3752 (FGSC 2489)	*mat A*; Oak Ridge
N3753 (FGSC 4200)	*mat a*; Oak Ridge
N4666	*mat a; suz12::*3xFLAG*::hph*
N4667	*mat unknown*; *suz12::*3xFLAG*::hph*
N4718	*mat a, set-7::hph*
N4729	*mat a; Δset-7::bar*
N4731	*mat A, Δset-7::bar; Δmus52::hph*
N4828	*mat a; eed::*3xFLAG*::hph*
N4830	*mat A; eed::*3xFLAG*::hph; Δmus52::bar*
N5808	*mat a; NCU07152::nat-1*
N5809	*mat A; NCU07152::nat-1; Δset-7::bar*
N7949	*mat a; NCU05173::hph; NUC07152::nat, his-3, sad-1?, set-7^{F247L}*
N8157	*mat A; set-7$^{1-853}$::*3xFLAG*::hph; Δmus52::bar*
N8158	*mat A; set-7$^{1-853}$::*3xFLAG*::hph; Δmus52::bar*
N8159	*mat A; set-7$^{1-853;\ Y833F}$::*3xFLAG*::hph; Δmus52::bar*
N8160	*mat A; set-7$^{1-853;\ Y833F}$::*3xFLAG*::hph; Δmus52::bar*
N8161	*mat A; set-7^{Y833F}::*3xFLAG*::hph; Δmus52::bar*
N8162	*mat A; set-7^{Y833F}::*3xFLAG*::hph*
N8163	*mat a; set-7^{H791A}::*3xFLAG*::hph; Δmus52::bar?*
N8164	*mat a; set-7^{H791A}::*3xFLAG*::hph; Δmus52::bar?*
N8165	*mat A; set-7^{Y833F}::*3xFLAG*::hph*
N8166	*mat A; set-7^{Y833F}::*3xFLAG*::hph; NCU07152::nat-1*
N8167	*mat A; set-7^{Y833F}::*3xFLAG*::hph; NCU07152::nat-1*
N8168	*mat A; set-7^{Y833F}::*3xFLAG*::hph; NCU07152::nat-1*
N8169	*eed::*3xFLAG*::hph; Δset-7::bar*
N8170	*eed::*3xFLAG*::hph; Δset-7::bar; Δmus52::bar*
N8171	*mat A; suz12::*3xFLAG*::hph; Δset-7::bar*
N8172	*mat a; suz12::*3xFLAG*::hph; Δset-7::bar*

N8173	*mat a; eed::*3xFLAG*::hph; set-7*^{Y833F}*::*3xFLAG*::hph; Δmus52::bar*
N8174	*mat a; eed::*3xFLAG*::hph, set-7*^{Y833F}*::*3xFLAG*::hph*
N8175	*mat A; suz12::*3xFLAG*::hph; set-7*^{Y833F}*::*3xFLAG*::hph*
N8176	*mat A; suz12::*3xFLAG*::hph; set-7*^{Y833F}*::*3xFLAG*::hph*
N8177	*mat A; set-7*$^{1\text{-}835;\ H791A}$*::*3xFLAG*::hph; Δmus52::bar*
N8178	*mat A; set-7*$^{1\text{-}835;\ H791A}$*::*3xFLAG*::hph*

Table 2: Primers for *set-7* truncation and catalytic-null constructs

Primer	**Description**	**Sequence (5'->3')**
4108	*set-7*_ORF_FP	GCCAACTTCCAGCCTTTCAC
4109	*set-7*_ORF_RP	CTCCTCCTCGTTCCGATATC
4110	*set-7*_3'UTR_FP	GTATTTGACTCGTGATTCTAGATATC
4111	*set-7*_3'UTR_RP	GCATCACCCACTACACGACA
2955	*hph*_RP	TCGCCTCGCTCCAGTCAATGACC
2954	*hph*_FP	AAAAAGCCTGAACTCACCGCGACG
6469	*set-7*_ORF_FP	CTCAAGGCTCAATGCGTGGT
6470	*set-7*$^{1\text{-}853}$_OFR_RP	CCTCCGCCTCCGCCTCCGCCGCCTCCGCCCGCCATC
6562	*set-7*^{H791A}_RP	TTCCGAGGCAGCGTTGATGTACC
6561	*set-7*^{H791A}_FP	GGTACATCAACGCTGCCTCGGAA
6564	*set-7*^{Y833F}_RP	GTTGTCGCCGAAGTTGAAGAAGAGC
6563	*set-7*^{Y833F}_FP	GCTCTTCTTCAACTTCGGCGACAAC
5611	*hph_nat-1*_RP	GCTCCAGCCAAGCCCAAAAAA
1231	*set-7*_ORF_FP	GTGGTATGCAAGGGATGTGGAGCG

Table 3: Plasmid for insertion of 3xFLAG::*hph* cassette

Plasmid	**Description**
2409	3xFLAG::*hph*

Table 4: Primers for Southern Analysis Genotyping

Primer	**Description**	**Sequence (5'->3')**
397	*hph*_RP	CGACGTCTGTCGAGAAGTT

2954	*hph*_FP	AAAAAGCCTGAACTCACCGCGACG

Table 5: Primers for RT-qPCR

Primer	**Description**	**Sequence (5'->3')**
3209	*NCU04173*_Actin_RTqPCR_FP	AATGGGTCGGGTATGTGCAA
3210	*NCU04173*_Actin_RTqPCR_RP	CTTCTGGCCCATACCGATCAT
6581	*NCU05173*_RTqPCR_FP	CGAGTGTGTTGGACCTGACG
6568	*NCU05173*_RTqPCR_RP	CCTGTTCGAGTTATCGGTGTTG
6583	*NCU07152*_RTqPCR_FP	GGTGACCCCAAACCTTATGTCGC
6584	*NCU07152*_RTqPCR_RP	GGCTCGAATCTGCCTCCAGC
6615	*NCU07624*_RTqPCR_FP	CCCAGGGGCGACAAGCAACC
6616	*NCU07624*_RTqPCR_RP	CAGAAATCATGTCAGCGCGTATGC
6613	*NCU09640*_RTqPCR_FP	CTCGTCTTTTATCTTGCACTTTACTTCC
6614	*NCU09640*_RTqPCR_RP	GCCAAAATGTGGTGATGAGCC
6271	*NCU02840*_RTqPCR_FP	CCCTCTCAGACGAGGATATTCA
6272	*NCU02840*_RTqPCR_RP	GCTCTGCTGCTTCTCCTTTAT

Glossary

Alternative splicing: the process in which a single gene can code for different proteins via differential expression of regions of the gene

Amino acids: molecules that are the building blocks of proteins. Lysine is the notable amino acid to this research

Chromatin: bundled nucleosomes, consisting of DNA and proteins

Conidia: asexual fungal spore

C-terminus: the end of an amino acid chain (polypeptide), terminating with a carboxyl (-COOH) group

Epigenetics: the study of heritable and semi-heritable changes in gene expression

Epitope: the part of an antigen protein to which an antibody binds

Heterochromatin: densely packed chromatin associated with gene regulation, specifically poor gene transcription

Histone: the proteins DNA wraps around. Histones have “tails” that can be modified, and these modifications influence DNA packaging

Homokaryons: common to fungus, the state in which a cell contains multiple, identical nuclei in the same cytoplasm

Mass spectrometry: an analytic technique that separates molecules based on mass; this is useful for identifying the size of a protein or determining protein and molecular interactions

Methylation: the addition of a methyl ($-CH_3$) group to an amino acid, such as the methylation of lysine 27 of histone H3. One, two, or three methyl groups can be deposited, and these marks are associated with gene repression

Nucleosome: bundle consisting of DNA wrapped around a histone protein core, composed of two of each of the four histones. Nucleosomes can be further bundled, forming chromatin

Orthologs: genes in different species that retain the same function

Post-translational modification: modifications to proteins, such as the covalent addition of functional groups, that alter protein function. Several modifications include acetylation, phosphorylation, and methylation

Reporter gene: a gene whose gene product indicates that transcription occurred

Repression: the mechanism for blocking expression of a gene

Silencing: the consequence of repression, in that repressed genes are “silent,” for they are not being expressed

References

1. Gross, D. S., Chowdhary, S., Anandhakumar, J., &Kainth, A. S. (2015). Chromatin. *Current Biology*, *25*(24), R1158-R1163.

2. Watson, J. D. (2004). *Molecular Biology of the Gene* (Vol. 1). Pearson Education India.

3. Bicocca, V. T., Ormsby, T., Adhvaryu, K. K., Honda, S., & Selker, E. U. (2018). ASH1-catalyzed H3K36 methylation drives gene repression and marks H3K27me2/3-competent chromatin. *Elife*, *7*, e41497.

4. Dillon, S. C., Zhang, X., Trievel, R. C., & Cheng, X. (2005). The SET-domain protein superfamily: protein lysine methyltransferases. *Genome Biology*, *6*(8), 227.

5. Jamieson, K., Wiles, E. T., McNaught, K. J., Sidoli, S., Leggett, N., Shao, Y., ... & Selker, E. U. (2016). Loss of HP1 causes depletion of H3K27me3 from facultative heterochromatin and gain of H3K27me2 at constitutive heterochromatin. *Genome Research*, *26*(1), 97-107.

6. Margueron, R., &Reinberg, D. (2011). The Polycomb complex PRC2 and its mark in life. *Nature*, *469*(7330), 343-349.

7. Wiles, E. T., & Selker, E. U. (2017). H3K27 methylation: a promiscuous repressive chromatin mark. *Current Opinion in Genetics &Development*, *43*, 31-37.

8. Ferrari, K. J., Scelfo, A., Jammula, S., Cuomo, A., Barozzi, I., Stützer, A., ... &Pasini, D. (2014). Polycomb-dependent H3K27me1 and H3K27me2 regulate active transcription and enhancer fidelity. *Molecular Cell*, *53*(1), 49-62.

9. van Mierlo, G., Veenstra, G. J. C., Vermeulen, M., & Marks, H. (2019). The complexity of PRC2 subcomplexes. *Trends in Cell Biology*.

10. Yuan, W., Wu, T., Fu, H., Dai, C., Wu, H., Liu, N., ... & Han, Z. (2012). Dense chromatin activates Polycomb repressive complex 2 to regulate H3 lysine 27 methylation. *Science*, *337*(6097), 971-975.

11. Healy, E., Mucha, M., Glancy, E., Fitzpatrick, D. J., Conway, E., Neikes, H. K., ... & Vermeulen, M. (2019). PRC2. 1 and PRC2. 2 synergize to coordinate H3K27 trimethylation. *Molecular Cell*, *76*(3), 437-452.

12. Jiao, L., & Liu, X. (2015). Structural basis of histone H3K27 trimethylation by an active polycomb repressive complex 2. *Science*, *350*(6258), aac4383.

13. Lavarone, E., Barbieri, C. M., &Pasini, D. (2019). Dissecting the role of H3K27 acetylation and methylation in PRC2 mediated control of cellular identity. *Nature Communications*, *10*(1), 1-16.

14. Squazzo, S. L., O'Geen, H., Komashko, V. M., Krig, S. R., Jin, V. X., Jang, S. W., ... &Farnham, P. J. (2006). Suz12 binds to silenced regions of the genome in a cell-type-specific manner. *Genome Research*, *16*(7), 890-900.

15. Laugesen, A., Højfeldt, J. W., &Helin, K. (2019). Molecular mechanisms directing PRC2 recruitment and H3K27 methylation. *Molecular Cell*, *74*(1), 8-18.

16. Hauri, S., Comoglio, F., Seimiya, M., Gerstung, M., Glatter, T., Hansen, K., ... &Beisel, C. (2016). A high-density map for navigating the human polycombcomplexome. *Cell Reports*, *17*(2), 583-595.

17. O'Carroll, D., Erhardt, S., Pagani, M., Barton, S. C., Surani, M. A., &Jenuwein, T. (2001). The polycomb-group GeneEzh2 is required for early mouse development. *Molecular and Cellular Biology*, *21*(13), 4330-4336.

18. Piunti, A., Hashizume, R., Morgan, M. A., Bartom, E. T., Horbinski, C. M., Marshall, S. A., ... &Misharin, A. V. (2017). Therapeutic targeting of polycomb and BET bromodomain proteins in diffuse intrinsic pontine gliomas. *Nature Medicine*, *23*(4), 493.

19. Varambally, S., Dhanasekaran, S. M., Zhou, M., Barrette, T. R., Kumar-Sinha, C., Sanda, M. G., ... & Rubin, M. A. (2002). The polycomb group protein EZH2 is involved in progression of prostate cancer. *Nature*, *419*(6907), 624-629.

20. Aramayo, R., & Selker, E. U. (2013). *Neurospora crassa*, a model system for epigenetics research. *Cold Spring Harbor Perspectives in Biology*, *5*(10), a017921.

21. Galagan, J. E., Calvo, S. E., Borkovich, K. A., Selker, E. U., Read, N. D., Jaffe, D., ... Rehman, B. (2003). The genome sequence of the filamentous fungus *Neurospora crassa. Nature*, *422*(6934), 859-868.

22. Honda, S., Bicocca, V. T., Gessaman, J. D., Rountree, M. R., Yokoyama, A., Eun, Y. Y., ... & Selker, E. U. (2016). Dual chromatin recognition by the histone deacetylase complex HCHC is required for proper DNA methylation in *Neurospora crassa*. *Proceedings of the National Academy of Sciences*, *113*(41), E6135-E6144.

23. Jani, K. S., Jain, S. U., Eva, J. G., Diehl, K. L., Lundgren, S. M., Müller, M. M., ... & Muir, T. W. (2019). Histone H3 tail binds a unique sensing pocket in EZH2 to activate the PRC2 methyltransferase. *Proceedings of the National Academy of Sciences*, *116*(17), 8295-8300.

24. Venkatesh, S., & Workman, J. L. (2015). Histone exchange, chromatin structure and the regulation of transcription. *Nature Reviews Molecular Cell Biology*, *16*(3), 178-189.

25. Wiles, E. T., McNaught, K. J., De Silva, S. M., Kaur, G., Selker, J. M., Ormsby, T., ... & Selker, E. U. (2019). Evolutionarily ancient BAH-PHD protein mediates Polycomb silencing. *bioRxiv*, 868117.

26. Kwon, T., Chang, J. H., Kwak, E., Lee, C. W., Joachimiak, A., Kim, Y. C., ... & Cho, Y. (2003). Mechanism of histone lysine methyl transfer revealed by the structure of SET7/9—AdoMet. *The EMBO Journal*, *22*(2), 292-303.

27. Jamieson, K., Rountree, M. R., Lewis, Z. A., Stajich, J. E., & Selker, E. U. (2013). Regional control of histone H3 lysine 27 methylation in Neurospora. *Proceedings of the National Academy of Sciences*, *110*(15), 6027-6032.

28. Klocko, A. D., Ormsby, T., Galazka, J. M., Leggett, N. A., Uesaka, M., Honda, S., ... & Selker, E. U. (2016). Normal chromosome conformation depends on subtelomeric facultative heterochromatin in *Neurospora crassa*. *Proceedings of the National Academy of Sciences*, *113*(52), 15048-15053.

29. Højfeldt, J. W., Laugesen, A., Willumsen, B. M., Damhofer, H., Hedehus, L., Tvardovskiy, A., ... &Helin, K. (2018). Accurate H3K27 methylation can be established de novo by SUZ12-directed PRC2. *Nature Structural &Molecular Biology*, *25*(3), 225-232.

30. Davis, R. H. (2000). *Neurospora: contributions of a model organism*. Oxford University Press.

31. Russo, V. E. A., Sommer, T., & Chambers, J. A. A. (1985). A modified Vogel's medium for crossings, mating-type tests and the isolation of female-sterile mutants of *Neurospora crassa*. *Fungal Genetics Reports*, *32*(1), 10.

32. Pomraning, K. R., Smith, K. M., & Freitag, M. (2009). Genome-wide high throughput analysis of DNA methylation in eukaryotes. *Methods*, *47*(3), 142-150.

33. Vollmer, S. J., &Yanofsky, C. (1986). Efficient cloning of genes of *Neurospora crassa*. *Proceedings of the National Academy of Sciences*, *83*(13), 4869-4873.

34. Miao, V. P., Freitag, M., & Selker, E. U. (2000). Short TpA-rich segments of the ζ-η region induce DNA methylation in *Neurospora crassa*. *Journal of Molecular Biology*, *300*(2), 249-273.